ISSN 0021-3640, JETP Letters, 2023, Vol. 117, No. 11, pp. 804–809. © The Author(s), 2023. This article is an open access publication.
ISSN 0021-3640, JETP Letters, 2023. © The Author(s), 2023. This article is an open access publication.
Russian Text © The Author(s), 2023, published in Pis'ma v Zhurnal Eksperimental'noi i Teoreticheskoi Fiziki, 2023, Vol. 117, No. 11, pp. 808–813.

OPTICS
AND LASER PHYSICS

Towards $\mathcal{PT}$-Symmetric Optical Dimer Fabrication without a Light-Absorbing Material

A. A. Dmitriev[a,*], K. V. Baryshnikova[a], and M. V. Rybin[a,b]

[a] *School of Physics and Engineering, ITMO University, St. Petersburg, 197101 Russia*
[b] *Ioffe Institute, St. Petersburg, 194021 Russia*
**e-mail: alexey.dmitriev@metalab.ifmo.ru*

Received March 30, 2023; revised April 17, 2023; accepted April 28, 2023

We consider an approach to engineer an optical dimer of particles operating in the spectral region near the dipolar resonance that exhibits parity–time symmetry-like features. Both particles are assumed to be made of a gain medium with the same refractive index and extinction coefficient. We suggest introducing a gain–loss contrast by altering the radiative loss of the particles through changing their shape. To demonstrate our approach, we consider a dimer of infinite filled and hollow cylinders. We demonstrate that a larger hollow diameter leads to a stronger radiative decay. Then we find the parameters of a dimer that has an exceptional point at a real frequency and exhibits two real eigenfrequencies when the gain–loss contrast is decreased.

DOI: 10.1134/S0021364023600945

During the last decade, a lot of research has been conducted in the field of non-Hermitian photonics [1–4]. The unintuitive physics that arises from the non-Hermiticity, such as the existence of real Hamiltonian eigenvalues in the systems that obey parity–time ($\mathcal{PT}$) symmetry, and the exceptional points where the Hamiltonian becomes degenerate (non-diagonalizable), leads to a plethora of optical effects, such as single mode lasing in a two-resonator setup [5], unidirectional transmission of light without reflection [6, 7], violation of reciprocity [8], and splitting of eigenfrequencies according to the root law when the degeneracy is lifted [9].

These effects have been successfully demonstrated in systems that are large compared to the wavelength, such as coupled waveguides, coupled ring and disk resonators, and flat layered structures. The non-Hermiticity is introduced by loss and gain from the medium absorption and stimulated emission under pumping, respectively [10], or by applying a spatially structured optical pumping to the gain medium [11]. To fabricate non-Hermitian metasurfaces with unique properties based on the $\mathcal{PT}$ symmetry and exceptional points, one needs to use resonant particles with a size comparable to, or smaller than the wavelength. In this case, application of spatially-structured optical pumping is hindered by the diffraction limit, while fabrication of metamaterials with a unit cell consisting of gain and lossy media requires a complex technological process.

Here, we consider the idea of shaping the resonators made of a gain medium to achieve a gain–loss contrast by increasing the radiative loss, allowing a $\mathcal{PT}$-symmetric metasurface design solely from a gain medium operating under uniform pumping. To demonstrate the approach, we chose the simplest system to analyze, that is a dimer of an infinite cylinder made of a dielectric gain medium, and an infinite hollow cylinder made of the same material, which is shown in Fig. 1. We consider the TE polarization, where the magnetic field vector is oriented along the cylinder axes. We demonstrate that the radiative loss becomes stronger when a hole is introduced, therefore it becomes possible to achieve a gain–loss contrast in a dimer made of the same material. Then we find the geometry of a dimer consisting of a cylinder and a hollow cylinder, that corresponds to an exceptional point, and analyze its eigenfrequencies and scattering spectra in the vicinity of the exceptional point.

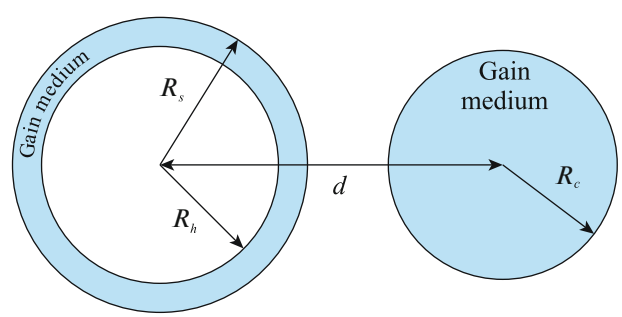

Fig. 1. (Color online) Sketch of the system studied, a dimer of a hollow cylinder and a filled cylinder.

$\mathcal{PT}$-symmetric and exceptional point photonics is conventionally studied in the framework of non-Hermitian two-level models well known from cavity quantum electrodynamics (QED), by assigning "levels" to the localized excitations in the resonators or waveguides [12]. Systems that are large compared to the wavelength, have been studied comprehensively and are well described by those models. However, despite the simplicity of the two-level model, rigorous treatment of the underlying electromagnetic wave propagation problem often appears to be quite complicated. The reason behind this complexity is that, in contrast to cavity quantum electrodynamics, where different kind of particles are coupled (e.g., excited electron and a photon being the levels and the coupling is carried by inter-level quantum transitions), in coupled resonators, levels and the coupling are essentially the same kind of excitation, namely, the electromagnetic field. This, in turn, leads to two consequences that complicate the problem.

The first one is that the energy exchange between the resonators is carried by electromagnetic waves involving retarded potentials. The coupling, in turn, becomes subject to these retardation effects. In photonics, the effective two-level Hamiltonian is defined as the time evolution operator of the system, so it becomes dependent on its own eigenvalue, i.e., the frequency. However, if the resonators are large compared to the wavelength, it is possible to treat them as waveguides, which have translation symmetry allowing to introduce a wave vector, which becomes the eigenvalue of the system master equation, instead of frequency.

The second complication is the existence of the radiative loss, making the losses and coupling inseparable. In waveguide-like structures, such as resonators operating on whispering gallery modes, the radiative losses are usually negligible, with the main loss channel usually being either scattering or absorption, allowing the coupled system to be treated by a two-level model. In contrast, when the size of the resonators is comparable to the wavelength, the radiative loss remains intertwined with the coupling [13].

Despite these difficuities, it is possible to formulate a two-level model using an approach based on the multiple scattering theory for coupled photonic resonators operating on the dipolar Mie resonance, however the effective Hamiltonian $\mathcal{H}$ turns out to be dependent on its own eigenvalue [13]:

$$\tilde{\omega}I - \mathcal{H} = \begin{bmatrix} \tilde{\omega} - \tilde{\omega}_c & i\Gamma_c H_0^{(1)}\left(\frac{\tilde{\omega}}{c}d\right) \\ i\Gamma_h H_0^{(1)}\left(\frac{\tilde{\omega}}{c}d\right) & \tilde{\omega} - \tilde{\omega}_h \end{bmatrix}, \quad (1)$$

where $\tilde{\omega}$ is the dimer complex eigenfrequency, $\tilde{\omega}_{c,h}$ are the scattering poles of each scatterer (a cylinder and a hollow cylinder) in the dimer and $\Gamma_{c,h}$ are the respective oscillator strengths, $H_0^{(1)}(x)$ is the Hankel function of the first kind which describes the dipole field in the 2D space, c is the lightspeed and d is the distance between the centers of the cylinders.

To describe the electromagnetic waves around the cylinders, we use the basis of multipoles that are described by the Bessel and Hankel functions. In this case, scattering on a cylinder is described by the Lorenz–Mie coefficients. For infinite cylinders of radius R_c, the scattering Lorenz–Mie coefficient can be expressed as

$$a_c = \frac{T_{21}^{(c)}}{T_{11}^{(c)}}, \quad (2)$$

where

$$T_{11}^{(c)} = H_l^{(1)}(x)J_l'(\tilde{n}x) - \tilde{n}H_l^{(1)\prime}(x)J_l(\tilde{n}x),$$

$$T_{12}^{(c)} = H_l^{(1)}(x)H_l^{(1)\prime}(\tilde{n}x) - \tilde{n}H_l^{(1)\prime}(x)H_l^{(1)}(\tilde{n}x),$$

$$T_{21}^{(c)} = \tilde{n}J_l'(x)J_l(\tilde{n}x) - J_l(x)J_l'(\tilde{n}x),$$

$$T_{22}^{(c)} = \tilde{n}H_l^{(1)}(\tilde{n}x)J_l'(x) - H_l^{(1)\prime}(\tilde{n}x)J_l(x),$$

$\tilde{n} = n + i\kappa$ is the cylinder refractive index, l is the azimutal number, which is equal to zero for dipoles, and $x = \tilde{\omega}R_c/c$.

The scattering poles are the points where the denominator of the 2D Lorenz–Mie dipole scattering coefficient becomes zero, i.e., $T_{11}^{(c)}(\tilde{\omega} = \tilde{\omega}_c) = 0$. By solving this equation for the $\tilde{\omega}_c$, we obtain the refractive index $\tilde{n}_c$ of the cylinder, which has a scattering pole at the frequency $\tilde{\omega}_c = \omega_c - i\gamma_c$. After that, the Lorenz–Mie coefficient can be approximated as

$$a_c \simeq \frac{-i\Gamma_c}{\tilde{\omega} - \tilde{\omega}_c}, \quad \Gamma_c = \lim_{\tilde{\omega}\to\tilde{\omega}_c} i(\tilde{\omega} - \tilde{\omega}_c)a_c, \quad (3)$$

in the vicinity of the scattering pole, where Γ_c is the oscillator strength.

Next, we consider a hollow cylinder, which can be treated as a core-shell particle. By matching the boundary conditions on the interfaces, one may arrive at the following formula for the scattering Lorenz–Mie coefficient of a hollow cylinder with a shell refractive index $\tilde{n}$, external radius R_c and internal radius R_h:

$$a_h = \frac{T_{21}^{(c)}T_{11}^{(h)} + T_{22}^{(c)}T_{21}^{(h)}}{T_{11}^{(c)}T_{11}^{(h)} + T_{12}^{(c)}T_{21}^{(h)}}, \quad (4)$$

where

$$T_{11}^{(h)} = \tilde{n}H_l^{(1)}(\tilde{n}\xi)J_l'(\xi) - H_l^{(1)\prime}(\tilde{n}\xi)J_l(\xi),$$

$$T_{12}^{(h)} = \tilde{n}H_l^{(1)}(\tilde{n}\xi)H_l^{(1)\prime}(\xi) - H_l^{(1)\prime}(\tilde{n}\xi)H_l^{(1)}(\xi),$$

$$T_{21}^{(h)} = J_l'(\tilde{n}\xi)J_l(\xi) - \tilde{n}J_l(\tilde{n}\xi)J_l'(\xi),$$

$$T_{22}^{(h)} = J_l'(\tilde{n}\xi)H_l^{(1)}(\xi) - \tilde{n}J_l(\tilde{n}\xi)H_l^{(1)}{}'(\xi),$$

and $\xi = \tilde{\omega}R_h/c$.

To find the scattering poles, we once again equate the denominator of the scattering coefficient to zero:

$$[T_{11}^{(c)}T_{11}^{(h)} + T_{12}^{(c)}T_{21}^{(h)}]\Big|_{\tilde{\omega}=\tilde{\omega}_h} = 0. \quad (5)$$

By solving this equation for $\tilde{\omega}_h$, we can obtain the shell refractive index $\tilde{n}$ and the hollow radius R_h, which correspond to a hollow cylinder having a scattering pole at the frequency $\tilde{\omega}_h = \omega_h - i\gamma_h$. Then the scattering coefficient a_h may be approximated in the vicinity of the pole in the same manner as in Eq. (3).

Let us study the dependence of the radiative loss with the hollow radius. Figure 2a,b show the dependences of the eigenfrequency ω_h and the eigenstate damping rate γ_h of hollow cylinders with various refractive indices on the diameter of the hollow, while Fig. 2c shows the corresponding oscillator strengths Γ_h. The losses can be seen to increase with increasing the hollow diameter. To distinguish between the increase of the radiative loss and the decrease of the gain medium volume, gain media ($\kappa < 0$, shown with solid and dashed lines), zero-loss zero-gain media ($\kappa = 0$, shown with dotted lines) and absorptive media ($\kappa > 0$, shown with dash-dotted lines) have been studied. In all three cases, the losses increase while the medium volume decreases, therefore this increase can be attributed to the radiative loss.

The increase in the radiative loss is accompanied by a frequency shift, as can be seen from Fig. 2a. As we are interested in introducing a gain–loss contrast without a frequency shift, a scale transformation should be applied to the hollow cylinder to alleviate the frequency shift.

Let us now analyze the eigenfrequencies of a dimer composed of a cylinder and a hollow cylinder. The Hamiltonian is dependent on its eigenvalues, making the equation for the eigenfrequency non-quadratic. Therefore, to find the dimer eigenfrequencies, one has to search for the zeros of the function $f(\tilde{\omega})$, which is defined as follows

$$f(\tilde{\omega}) = \det(\tilde{\omega}I - \mathcal{H}). \quad (6)$$

We search for the exceptional point, which is the point where two or more eigenfrequencies coalesce. Using a Taylor expansion, one may easily demonstrate that such a point $\tilde{\omega}_{\mathrm{EP}}$ satisfies the following conditions

$$\begin{cases} f(\tilde{\omega}_{\mathrm{EP}}) = 0, \\ f'(\tilde{\omega}_{\mathrm{EP}}) = 0. \end{cases} \quad (7)$$

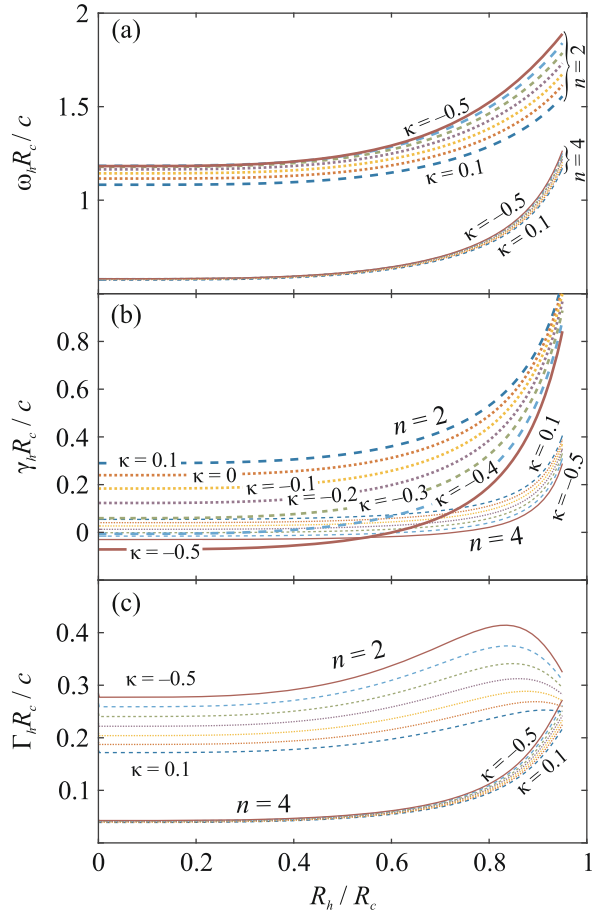

Fig. 2. (Color online) Dependences of the dipolar scattering pole of an infinite hollow cylinder made of a dielectric with a complex refractive index $\tilde{n} = n + i\kappa$ on the hollow radius (R_h), respective to the external radius (R_c): resonant frequency (a), resonant state damping rate (b) and oscillator strength (c). TE polarization, refractive indices $n = 2$ and $n = 4$, and extinction coefficients $\kappa = -0.5, -0.4, \ldots, +0.1$ considered.

Solving this equation system for the scattering poles $\tilde{\omega}_{c,h}$, one arrives at the following expression

$$\tilde{\omega}_{c,h} = \tilde{\omega}_{\mathrm{EP}} - A\Gamma_c\Gamma_h\left[\tau \pm \sqrt{\tau^2 + \frac{1}{\Gamma_c\Gamma_h}}\right], \quad (8)$$

where $A = H_0^{(1)}(\tilde{\omega}_{\mathrm{EP}}d/c)$ and $\tau = (d/c)H_1^{(1)}(\tilde{\omega}_{\mathrm{EP}}d/c)$. Using Eq. (8), one may find the scattering poles of the particles, which, placed at the distance d, will form a dimer that is at the exceptional point, i.e., only has one eigenmode at the frequency $\tilde{\omega}_{\mathrm{EP}}$ instead of a pair of eigenmodes at different frequencies.

Using Eq. (8), we find the scattering poles of a dimer that is expected to have an exceptional point at the frequency $\tilde{\omega} = 1.186c/R_c$ (which corresponds to the vacuum wavelength 530 nm and the cylinder radius $R_c = 100$ nm). We also fix the distance between

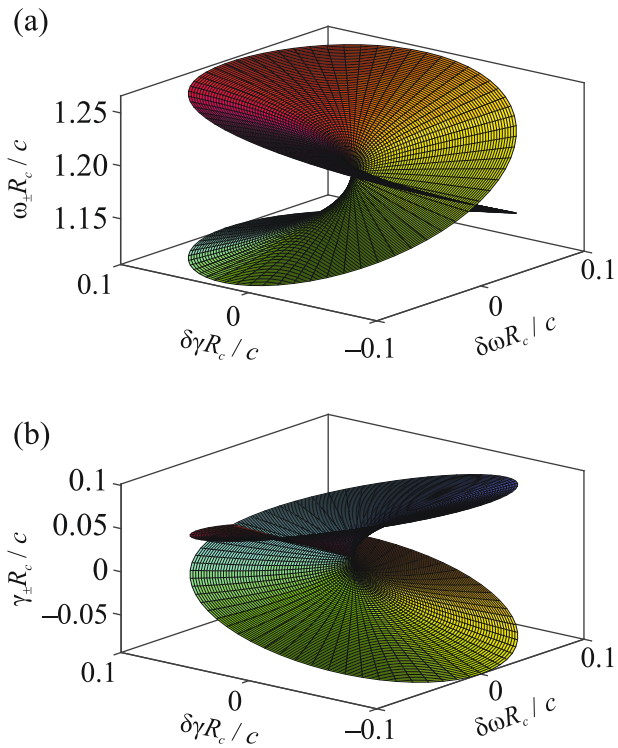

Fig. 3. (Color online) Eigenfrequencies of a dimer consisting of a hollow and filled cylinders, as the dependence of the complex detuning $\delta\omega - i\delta\gamma$ on the exceptional point: eigenmode frequency (a), eigenmode damping rate (b).

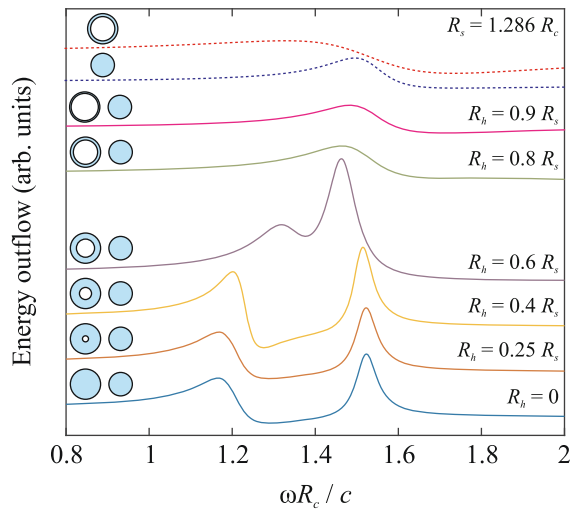

Fig. 4. (Color online) Spectra of the outflowing energy of the dimer of hollow (radius R_s) and filled (radius R_c) cylinders made of a gain medium with a refractive index $\tilde{n} = 1.99 - 0.488i$ illuminated by a plane wave, as dependences of the hollow radius (R_h). TE polarization.

the centers at $d = 4.65R_c$, which leads to a purely imaginary difference between the scattering poles, necessary for the $\mathcal{PT}$ symmetry regime. The following scattering poles are then found from Eq. (8): $\tilde{\omega}_c = (1.19 + 0.0642i)c/R_c$, which corresponds to $\tilde{n} = 1.99 - 0.488i$, and $\tilde{\omega}_h = (1.19 - 0.161i)c/R_c$. In order to match the frequencies ω_c and ω_h, the hollow cylinder has been upscaled, so that its external radius would become $R_s = 1.286R_c$, where R_c is the radius of the filled cylinder. The hollow radius corresponding to the scattering pole at $\tilde{\omega}_h$ is $R_h = 0.8R_s$. The oscillator strengths of the cylinders then become $\Gamma_c = 0.28$ and $\Gamma_h = 0.317$.

These values have been substituted into the effective Hamiltonian at Eq. (1). Then, to check if the system is indeed at the exceptional point, a symmetric frequency detuning $\delta\tilde{\omega} = \delta\omega - i\delta\gamma$ was introduced into the scattering poles given by Eq. (8): $\tilde{\omega}_c = (1.19 + 0.0642i)c/R_c + \delta\tilde{\omega}/2$, and $\tilde{\omega}_h = (1.19 - 0.161i)c/R_c - \delta\tilde{\omega}/2$. The eigenfrequencies $\tilde{\omega}_{\pm} = \omega_{\pm} - i\gamma_{\pm}$ of the Hamiltonian were then sought for, as the dependence of the complex detuning $\delta\tilde{\omega}$. The resulting eigenfrequency sheets, shown in Fig. 3, display the topology resemblant of the Riemann surface of a complex square root function, which is a characteristic feature of an exceptional point [1, 3, 4]. We also note that, when only the gain–loss contrast is varied ($\delta\omega = 0$), a behavior similar to the $\mathcal{PT}$ symmetry is observed. When the gain–loss contrast is decreased compared to its value at the exceptional point, the dimer has two purely real eigenfrequencies. Increasing the gain–loss contrast, in turn, leads to the $\mathcal{PT}$ symmetry breaking-like behavior, where a damped ($\gamma_{\pm} < 0$) and an amplifying ($\gamma_{\pm} > 0$) modes exist at the same frequency ($\omega_{\pm} = \omega_{EP}$). We, however, note, that the dimer itself does not possess the $\mathcal{PT}$ symmetry in the rigorous sense: because of a different geometry of the scatterers (a filled and a hollow cylinder), the composition of a parity and a time inversion transformations would yield a different system compared to the dimer considered.

Finally, we consider the scattering spectra on the dimer made of a gain medium with a refractive index $n = 1.99$ and the extinction coefficient $\kappa = -0.488$, consisting of a cylinder with a radius R_c and a hollow cylinder with the external radius $R_s = 1.286R_c$. To obtain the scattering spectra, we use the multiple scattering theory described elsewhere [13–24], considering only the dipolar contribution. The excitation is a plane wave with an incidence direction normal to the plane passing through the axes of the cylinders. As the dimer is made of a gain material and exists at a radiant regime, we consider the outflowing energy, which we define as the extinction cross-section taken with the negative sign. The spectra are shown in Fig. 4 as a dependence of the hole radius. Decreasing the hole size leads to a decrease in the gain–loss contrast, which is accompanied by a small eigenfrequency shift.

This leads to a stronger coupling compared to the exceptional point, which leads to a frequency splitting. Increasing the hollow radius corresponds to an increase in the gain–loss contrast, which leads to the $\mathcal{PT}$ symmetry breaking. In this regime, the eigenmodes exist separately in the cylinder, which encompasses a radiant mode, and in the hollow cylinder, which has a decaying mode at the same frequency.

CONCLUSIONS

We have considered infinite dielectric cylinders with hollows and demonstrated that the radiative losses increase with increasing hollow diameter. This dependence allowed us to achieve a gain–loss contrast between a hollow cylinder and a cylinder without a hole made of the same material. Using the dipole approximation, we derived the equations for the geometric parameters of a dimer consisting of a cylinder and a hollow cylinder, that has an exceptional point at a given frequency. By selecting a purely real exceptional point frequency and a distance that corresponds to a purely imaginary difference between the scattering poles of the solid and hollow cylinder, we were able to construct a dimer with a $\mathcal{PT}$ symmetry-like behavior. With decreasing gain–loss contrast, this dimer displays two purely real eigenfrequencies, while increasing the gain–loss contrast leads to the appearance of a damping and an amplifying mode at the same frequency. We have analyzed the scattering spectra of the dimers of the solid cylinder and a cylinder with varied hollow diameter and demonstrated that decreasing the gain–loss contrast by decreasing the hollow diameter leads to emergence of a splitting of the resonance in the spectra.

Our findings might be useful for designing the metasurfaces operating almost at the $\mathcal{PT}$ symmetry and exceptional point regimes. We admit that the negative imaginary part of the refractive index as large as $\kappa = -0.5$, that is required for our dimer to exhibit the $\mathcal{PT}$ symmetry-like behavior, can not be realized in optical gain media, which are currently limited by $\kappa \sim 10^{-2}$. Such a strong gain is required to compensate the strong radiative decay of the dipole resonances. At the same time, the radiative losses, if not compensated, will overwhelm the loss contrast, making the $\mathcal{PT}$ symmetry effects impossible to observe. Therefore, considering the geometric resonances of a higher order, such as quadrupole or octopole states, which are characterized by a higher quality factor, seems to be a way to alleviate this problem. In particular, halide perovskites might be a suitable gain medium, as the compensation of the radiative losses in quadrupole and octopole states by gain, leading to single-particle lasing, has been experimentally demonstrated on this platform [25].

We considered infinite cylinders due to the simplicity of analysis. To fabricate real structures one would need particles with finite sizes, such as finite cylinders. Hollow core waveguides can be used for implementation in the terahertz range, as their technology of fabrication with the diameters as small as 10 μm is well established [26]. In optical range one may use hollow cylinders fabricated by electron beam lithography, which may have a radius as small as 100 nm. Heights of such cylinders can exceed the radius by several times [27]. However, in this case the resonance frequency is shifted from the value predicted by Mie theory (about 10% for the cylinder height being equal to three times the radius [28]) due to the coupling between the Mie modes and the Fabry–Perot modes in the cylinder, so one would have to take extra steps to treat this shift.

FUNDING

This work was supported by the Russian Science Foundation (project no. 21-79-10190).

CONFLICT OF INTEREST

The authors declare that they have no conflicts of interest.

OPEN ACCESS

REFERENCES

1. R. El-Ganainy, K. G. Makris, M. Khajavikhan, Z. H. Musslimani, S. Rotter, and D. N. Christodoulides, Nat. Phys. **14**, 11 (2018).
2. L. Feng, R. El-Ganainy, and L. Ge, Nat. Photon. **11**, 752 (2017).
3. M.-A. Miri and A. Alù, Science (Washington, DC, U. S.) **363**, eaar7709 (2019).
4. Ş. K. Özdemir, S. Rotter, F. Nori, and L. Yang, Nat. Mater. **18**, 783 (2019).
5. L. Feng, Z. J. Wong, R.-M. Ma, Y. Wang, and X. Zhang, Science (Washington, DC, U. S.) **346**, 972 (2014).
6. Z. Lin, H. Ramezani, T. Eichelkraut, T. Kottos, H. Cao, and D. N. Christodoulides, Phys. Rev. Lett. **106**, 213901 (2011).

7. L. Feng, X. Zhu, S. Yang, H. Zhu, P. Zhang, X. Yin, Y. Wang, and X. Zhang, Opt. Express **22**, 1760 (2013).
8. L. Feng, M. Ayache, J. Huang, Y.-L. Xu, M.-H. Lu, Y.-F. Chen, Y. Fainman, and A. Scherer, Science (Washington, DC, U. S.) **333**, 729 (2011).
9. K. J. H. Peters and S. R. K. Rodriguez, Phys. Rev. Lett. **129**, 013901 (2022).
10. B. Peng, Ş. K. Özdemir, F. Lei, F. Monifi, M. Gianfreda, G. L. Long, S. Fan, F. Nori, C. M. Bender, and L. Yang, Nat. Phys. **10**, 394 (2014).
11. H. Hodaei, A. U. Hassan, S. Wittek, H. Garcia-Gracia, R. El-Ganainy, D. N. Christodoulides, and M. Khajavikhan, Nature (London, U.K.) **548**, 187 (2017).
12. A. F. Kockum, A. Miranowicz, S. D. Liberato, S. Savasta, and F. Nori, Nat. Rev. Phys. **1**, 19 (2019).
13. A. A. Dmitriev and M. V. Rybin, Phys. Rev. A **99**, 063837 (2019).
14. A. Egel, L. Pattelli, G. Mazzamuto, D. S. Wiersma, and U. Lemmer, J. Quant. Spectrosc. Radiat. Transfer **199**, 103 (2017).
15. D. Felbacq, G. Tayeb, and D. Maystre, J. Opt. Soc. Am. A **11**, 2526 (1994).
16. K. M. Leung and Y. Qiu, Phys. Rev. B **48**, 7767 (1993).
17. P. Lloyd and P. Smith, Adv. Phys. **21**, 69 (1972).
18. P. Markoš and V. Kuzmiak, Phys. Rev. A **94**, 033845 (2016).
19. P. Markoš, Opt. Commun. **361**, 65 (2016).
20. E. E. Maslova, M. F. Limonov, and M. V. Rybin, Opt. Lett. **43**, 5516 (2018).
21. A. Moroz, J. Phys.: Condens. Matter **6**, 171 (1994).
22. N. A. Nicorovici, R. C. McPhedran, and L. C. Botten, Phys. Rev. E **52**, 1135 (1995).
23. G. Tayeb and S. Enoch, J. Opt. Soc. Am. A **21**, 1417 (2004).
24. X. Wang, X.-G. Zhang, Q. Yu, and B. Harmon, Phys. Rev. B **47**, 4161 (1993).
25. E. Tiguntseva, K. Koshelev, A. Furasova, P. Tonkaev, V. Mikhailovskii, E. V. Ushakova, D. G. Baranov, T. Shegai, A. A. Zakhidov, Y. Kivshar, and S. V. Makarov, ACS Nano **14**, 8149 (2020).
26. F. Yu, W. J. Wadsworth, and J. C. Knight, Opt. Express **20**, 11153 (2012).
27. Z.-B. Fan, H.-Y. Qiu, H.-L. Zhang, X.-N. Pang, L.-D. Zhou, L. Liu, H. Ren, Q.-H. Wang, and J.-W. Dong, Light Sci. Appl. **8**, 67 (2019).
28. M. V. Rybin, K. B. Samusev, P. V. Kapitanova, D. S. Filonov, P. A. Belov, Y. S. Kivshar, and M. F. Limonov, Phys. Rev. B **95**, 165119 (2017).